

663292
DP-1273

AEC RESEARCH AND DEVELOPMENT REPORT

IRRADIATION GROWTH OF EBR-II FUEL PINS

E. F. STURCKEN

G. G. WICKS



SRL
RECORD COPY

Savannah River Laboratory

Aiken, South Carolina

NOTICE

This report was prepared as an account of work sponsored by the United States Government. Neither the United States nor the United States Atomic Energy Commission, nor any of their employees, nor any of their contractors, subcontractors, or their employees, makes any warranty, express or implied, or assumes any legal liability or responsibility for the accuracy, completeness or usefulness of any information, apparatus, product or process disclosed, or represents that its use would not infringe privately owned rights.

Printed in the United States of America
Available from
National Technical Information Service
U. S. Department of Commerce
5285 Port Royal Road
Springfield, Virginia 22151
Price: Printed Copy \$3.00; Microfiche \$0.95

663292
DP-1273

Metals, Ceramics, and Materials
(TID-4500, UC-25)

IRRADIATION GROWTH OF EBR-II FUEL PINS

by

E. F. Sturcken
G. G. Wicks*

Approved by

R. T. Huntoon, Research Manager
Nuclear Materials Division

December 1971

* On educational leave of absence at:

Metallurgy and Materials Science Dept.
Massachusetts Institute of Technology
Cambridge, Massachusetts

E. I. DU PONT DE NEMOURS & COMPANY
SAVANNAH RIVER LABORATORY
AIKEN, S. C. 29801

CONTRACT AT(07-2)-1 WITH THE
UNITED STATES ATOMIC ENERGY COMMISSION

ABSTRACT

Preferred orientation studies of centrifugally bonded EBR-II fuel pins showed that the pins have a [110], [001] axial texture, which is responsible for their shortening in length and diametrical growth during irradiation. The growth indices calculated from texture data correlate well with observed irradiation growth and give a single crystal growth rate, g , of 200% per % burnup, which is in the range measured for other uranium alloys.

Texture gradient studies showed that the texture forms during centrifugal bonding as a stress-relieving mechanism for the $\gamma \rightarrow \alpha$ transformation.

CONTENTS

	<u>Page</u>
Introduction	5
Summary	7
Discussion	9
X-ray Diffraction Studies of Fuel Pins	9
Experimental and Analytical Procedures	14
Results and Conclusions	14
Axial Texture Gradient Measurements	18
Texture Measurements on End Sections and Composite Specimens	20
Effects of Electropolishing Solution on Texture Measurements	22
Line Broadening and Lattice Contraction	21
Microstructure and Hardness of Fuel Pins	22
Experimental Procedure	22
Results	22
Hardness Measurements	22
Microstructure Studies	23
Electron Probe Micro-Analysis	29
Mechanism for Stress-Induced Texture	29
Texture Profiles	29
Source of Stress	29
Magnitude of Stress	31
Direction of Stress	31
Other Mechanisms for Stress-Induced Texture	31
Acknowledgments	31
References	32

LIST OF TABLES AND FIGURES

<u>Table</u>	<u>Page</u>
I Comparison of Random Diffraction Intensities from EBR-II Fuel Pin 12367 and Pure Uranium	11
II Texture Measurements of Bottom-End Sections of EBR-II Fuel Pins	19
III DPH Values for Uranium-Fissium Fuel Pins	30

<u>Figure</u>		
1	Composite Sample Consisting of Transverse Sections of an EBR-II Fuel Pin	9
2	Experimental Arrangement for Texture Measurements of EBR-II Fuel Pins	10
3	Typical Diffraction Profiles for Bottom End of Centrifugally Bonded and Impact-Bonded EBR-II Fuel Pins	13
4	Compressive Stress During Heat Treatment of a Centrifugally Bonded Pin	14
5	Diametrical Irradiation Growth of Centrifugally Bonded Fuel Pins	15
6	Texture Gradient in Centrifugally Bonded Fuel Pin .	15
7	Growth Rate and Growth Index for Centrifugally Bonded Fuel Pins	17
8	Effect of Electropolish on Diffraction Intensities of EBR-II Fuel Pins	21
9	Optical Micrographs of Impact-Bonded Fuel Pin . . .	24
10	Optical Micrographs of Centrifugally Bonded Fuel Pin	25
11	Scanning Electron Micrographs of Impact-Bonded Fuel Pin	26
12	Scanning Electron Micrograph of Centrifugally Bonded Fuel Pin	27
13	Replica Micrographs of Grain Boundary and Matrix Structure of Impact-Bonded and Centrifugally Bonded Pins	28
14	Variation of Texture Along the Length of Centrifugally Bonded Pins	30

INTRODUCTION

The Savannah River Laboratory assisted Argonne National Laboratory (ANL) in determining the cause of shortening that occurs during irradiation of Experimental Breeder Reactor (EBR-II) fuel elements manufactured by employing a centrifugal bonding process. The length shortening and corresponding diameter increases were in some cases as high as 10% per % burnup.¹

Density and metallography measurements on irradiated EBR-II fuel elements at Battelle-Northwest showed that no swelling, except that due to fission fragments, occurred.² Preliminary qualitative X-ray preferred orientation (texture) studies³ of the alpha uranium triplet showed that the I(110)/I(021) ratio for a centrifugally bonded pin was greater than expected for random orientation. Hence, it was suspected that the dimensional changes were caused by anisotropic irradiation growth⁴ due to texture of the alpha uranium.

At the request of ANL, SRL carried out preferred orientation studies with the following objectives: 1) develop a method for characterizing texture in EBR-II fuel pins; 2) characterize the texture of fuel pins, which received special heat treatments to improve their irradiation performance; and 3) measure the axial texture profile of a centrifugally bonded pin, and correlate the variation of texture with the variation in diametrical irradiation growth along the length of the pin. The completed work is described in this report.

The EBR-II fuel element is a pin (0.15-in. dia. by 13.5-in. long) of uranium-base alloy, called uranium-fissium (Fs),^{5,6} i.e., enriched uranium plus 2-2.5 wt % each of molybdenum and ruthenium, 0.01-0.3 wt % each of rhodium, palladium, zirconium, and niobium, and 100-300 ppm each of iron, silicon, and nickel. The alloy composition is normally referred to as U-5 wt % Fs and was chosen to correspond to the composition that is predicted to result after pyrometallurgical reprocessing of spent uranium fuel.

Originally the fuel elements were made at ANL. The fuel pins were injection cast and then canned in a stainless steel jacket with a sodium bond. Sodium bonding was performed at ANL by heating the jacketed elements to 500°C and impacting them 1000 to 2000 times with a pneumatically driven "impact" cylinder to assure that sodium had completely filled the space between the stainless steel jacket and the fuel pins. During bonding the uranium-fissium alloy is transformed from a distorted bcc gamma uranium phase to a distorted orthorhombic alpha uranium phase. These fuel elements were stable during irradiation in the EBR-II.

Fuel element manufacturing was later contracted to a vendor for routine production. The vendor used the same casting process, but bonded with sodium by centrifuging the pins at 720 rpm at 482°C. The centrifuge process was used instead of impact bonding for production economy. Fuel elements fabricated by centrifugal bonding shortened in length and increased in diameter during irradiation.

SUMMARY

Preferred orientation studies of EBR-II (U-5 wt % Fs) fuel pins showed that pins cast and centrifugally bonded have a [110], [001] axial texture, which is responsible for their shortening in length and diametrical growth during irradiation.

The growth indices⁷ calculated from texture data correlate well with observed irradiation growth and give a single crystal growth rate,⁸ g, of 200% per % burnup, which is in the range measured for other uranium alloys.^{9,10}

The observed growth also correlates well with the diffraction intensity ratio $I(110)/I(021)$. Hence, this ratio can be measured, nondestructively, on the ends of fuel pins and serve as a rapid method of texture control.

Texture gradient studies showed that the texture is caused by compressive stress from the centrifuge during bonding. The texture is maximum at the bottom end of the pin where the stress is 3000 psi and is reduced to a negligible value about 9 in. from the bottom where the stress is reduced to 1000 psi.

The texture is believed to form during bonding as a stress-relieving mechanism for the $\gamma \rightarrow \alpha$ transformation. Two possible mechanisms are: 1) centrifuge stresses cause the grains to orient, during nucleation and growth of the alpha phase, such that the weaker bonds of the [010] direction are parallel to the direction of tensile stress, or 2) the centrifuge stresses may cause the grains to slip on only one or two sets of planes during the $\gamma \rightarrow \alpha$ transformation, and thereby generate the texture.

Microstructure studies using scanning and replica electron microscopy showed that the pins bonded by both methods have the appearance of a two-phase structure, even though micro-hardness and X-ray measurements showed both structures to be alpha uranium. The X-ray measurements also showed that the diffraction lines are broadened, the lattice is contracted 0.05Å in the [010] direction, and the grain boundary alpha phase is less textured than the matrix alpha phase. Previous studies¹¹ of distorted alpha phase formed from other metastable gamma phase uranium alloys attribute these differences in metallographic appearance to $\gamma \rightarrow \alpha$ transformation both by shear and by nucleation plus growth mechanisms.

(Blank)

DISCUSSION

X-RAY DIFFRACTION STUDIES OF FUEL PINS

Experimental and Analytical Procedures

The X-ray diffraction measurements of texture were performed on specimens prepared by two sampling methods: 1) twenty-four transverse sections of a fuel pin were mounted to form a composite specimen (Figure 1), representing 2/3 the length of the pin, and 2) axial texture gradient measurements were made on single transverse sections taken at various distances along the length of the pin.

The specimens were ground by standard procedures through 1/4-u diamond abrasive and electropolished to remove worked metal. The electropolishing was performed in a solution of 200 ml ethyl alcohol, 125 ml H_3PO_4 , and 125 ml ethylene glycol. The electropolishing conditions were: stainless steel cathode, 18 volts, 0.3 to 0.6 amps for 20 sec. Although this electropolishing solution is a standard one for uranium, it preferentially attacks the region around the grain boundaries in uranium-fissium. Therefore, the effect of this attack on the X-ray results was studied by electropolishing one specimen in a solution¹² of one part of 118 g CrO_3 in 100 ml H_2O to four parts glacial acetic acid, which attacks the structure uniformly.

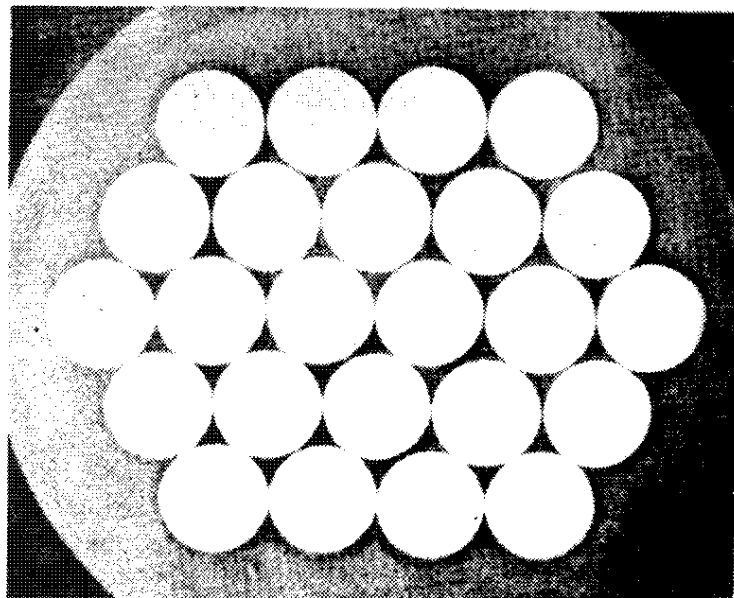
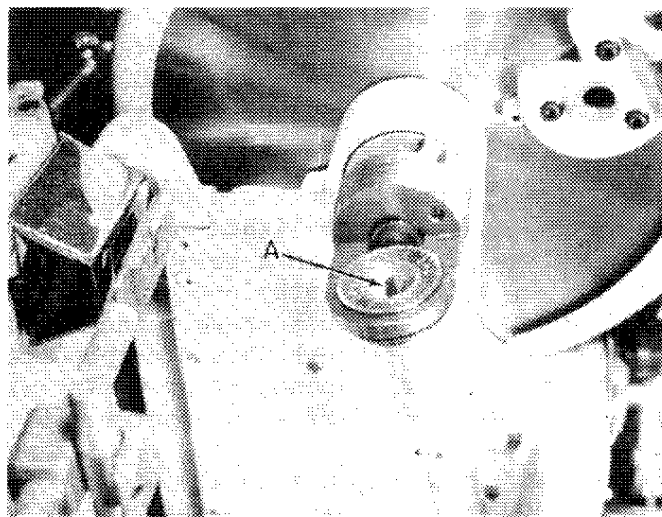
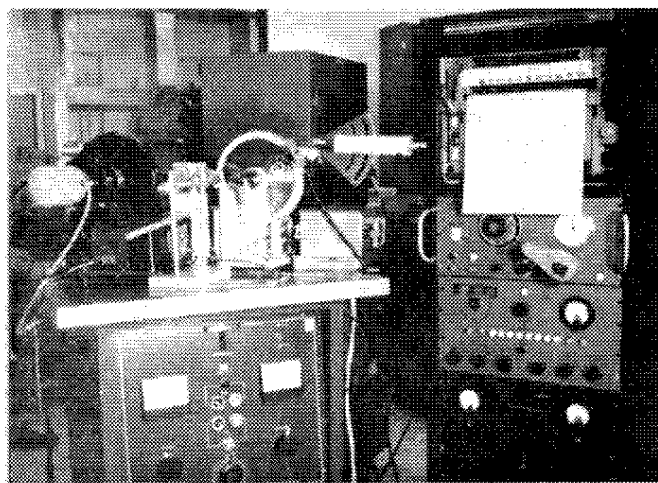


FIGURE 1 Composite Sample Consisting of Transverse Sections of an EBR-II Fuel Pin (4X)

The specimens were scanned on a conventional North American Philips diffractometer (Figure 2), with a fine focus $\text{CuK}\alpha$ X-ray tube and a rotating specimen holder. An Advanced Metals Research Model 3-202 monochromator with a graphite single crystal was used on the detector side of the diffractometer. A special cup-shaped specimen holder¹³ was used for the texture gradient measurements.



a. Fuel Pin (A) Mounted in Norelco Rotating Specimen Holder



b. X-ray Diffraction Equipment

FIGURE 2 Experimental Arrangement for Texture Measurements of EBR-II Fuel Pins

The preferred orientation measurements were made by the inverse pole figure method.¹⁴ In this method the orientation is described by the quantity, P_{hkl} , where

$$P_{hkl} = I_{hkl}/I_{hkl}^0 \div 1/n \sum_{hkl} I_{hkl}/I_{hkl}^0$$

where

n = number of planes

I_{hkl} = the diffraction intensity from the plane (hkl)

I_{hkl}^0 = the calculated intensity for the plane (hkl)
from a specimen with a random orientation

Thus, $P_{hkl} = 1$ for random orientation, and $P_{hkl} > 1$ for an excess of a given orientation. Calculated random intensities¹⁵ were used for the composite specimens. The random intensities could not be calculated for single transverse sections because the X-ray beam area was larger than the specimen so a random standard was prepared from Pin 12367 that was injection cast, heat treated at 660°C for 1-1/2 hr, and impact bonded. The measured standard intensities compared reasonably well with previous measurements¹³ (Table I) on a cross section of 1/8-in.-diameter rod machined from an unalloyed uranium plate that was prepared by powder metallurgical methods. There should be some differences between uranium and uranium-fissium because of the strained state of uranium-fissium and the small differences in atomic scattering factors due to alloying constituents.

TABLE I

Comparison of Random Diffraction Intensities from
EBR-II Fuel Pin 12367 and Pure Uranium

Middle of EBR-II Fuel Pin		Unalloyed Uranium Rod ^b
hkl	I_{hkl}^0 ^a	I_{hkl}^0
(110)	0.79	0.70
(021)	1.00	1.00
(002)	0.59	0.50
(111)	0.74	0.69
(112)	0.89	0.76
(131)	0.88	0.70
(133)	0.53	0.37
(114)	0.35	0.24

a. $GI = +0.0002$ for the I_{hkl}^0 of Pin 12367 assuming the pure uranium I_{hkl}^0 are the random standards. The bottom end of the fuel pin had an average value of $GI = -0.02$, and the top end an average value of $GI = +0.04$.

b. This was a 1/8-in. rod of pure uranium prepared by powder metallurgy techniques (described in Reference 13).

The tendency for the specimen to grow or shorten during irradiation is expressed by the growth index,⁷ GI, given by the equation

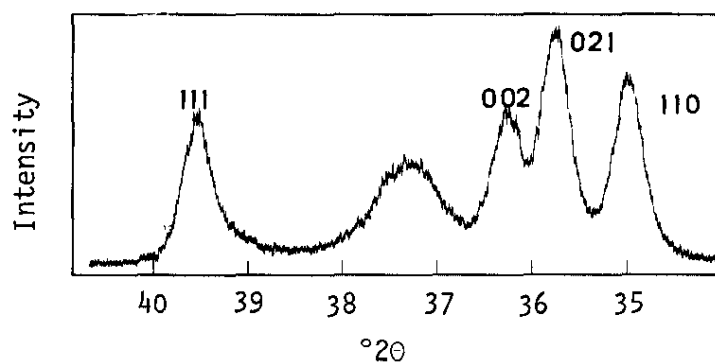
$$GI = \sum_{hkl} (P_{hkl} - 1)(\cos^2 \beta_{hkl} - \cos^2 \alpha_{hkl})$$

where α_{hkl} and β_{hkl} are, respectively, the angles which the pole of the plane (hkl) makes with the "a" and "b" crystallographic axes. More refined forms of the growth index expression are available^{14,16} that take into account the asymmetrical distribution of measured diffraction planes; however, the precision of the measurements did not merit their use in this study.

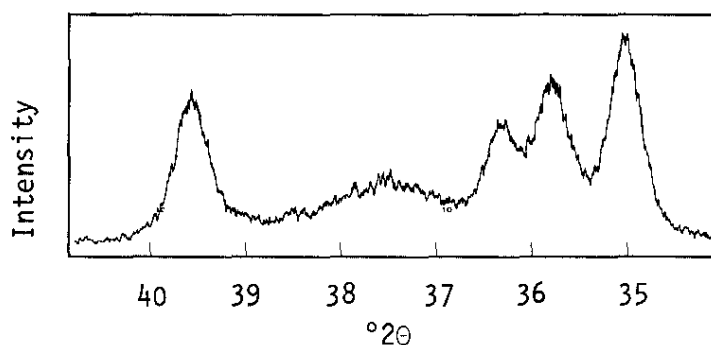
The uranium-fissium alloy gives a very complex diffraction pattern because the peaks from the predominant phase, alpha uranium, are broadened, shifted, and overlapped due to lattice strain, and they generally contain contributions from the minor phases in the alloy, namely U_2Ru , U_2Mo , and possibly distorted gamma-phase uranium. About 70 alpha uranium peaks and 15 unknown peaks were observed; however, only about eight alpha uranium peaks were found suitable for the preferred orientation measurements, namely (110), (021), (002), (111), (112), (131), (133), and (114).

The diffraction intensities were estimated from planimeter measurements of the areas of the peaks on the strip chart records. Special care was exercised to resolve the (110), (021), (002) triplet before planimetry, since the (021) and (110) are the most important peaks (Figure 3) for determining the preferred orientation. The contraction of the uranium-fissium lattice in the [010] direction displaces the (021) peak toward the (002) peak, making the overlap with the (002) greater than in pure uranium. Furthermore, the (021) is always broader because of the contribution from the (002) and the (110) peaks. The (002) is also distorted by contributions from the broad peak between 36.5° and 38.5° (Figure 3). There are allowed reflections in this 2θ region from U_2Ru , U_2Mo and gamma uranium, so it was not possible to identify which phase or phases cause the broad peaks.

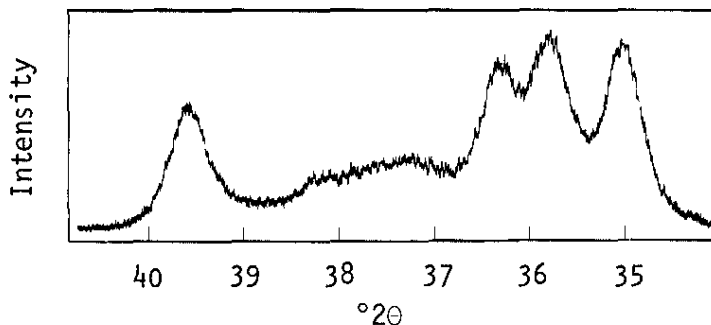
A computer program was written to determine the peak areas by curve fitting the peaks with a Gaussian distribution function. The program gave good results for impact-bonded fuel pins, and also for specially heat treated centrifugally bonded pins because they have relatively strain-free, over-aged structures. However, the program gave poor results for centrifugally bonded pins because the peaks were too distorted in shape to fit a Gaussian distribution function.



a. Impact-Bonded Pin 049H23



b. Centrifugally Bonded Pin 02112 (large-grained end)



c. Centrifugally Bonded Pin 01776 (small-grained end)

FIGURE 3 Typical Diffraction Profiles for Bottom End of Centrifugally Bonded and Impact-Bonded EBR-II Fuel Pins

Note that the (021) is at 35.75° ; its position in pure uranium is 35.55° . The centrifugally bonded pins have broader diffraction lines (b, c) than the impact-bonded pins (a). The $I(110)/I(021)$ ratio is larger in b than in c. The unknown peak next to the triplet is probably U_2Ru , U_2Mo and residual γ uranium; this peak is better developed for the impact-bonded pin.

The best method found for resolving the (110), (021), (002) triplet follows: Start with the low angle half of the (110) peak and assume it is a perfect "half peak." Sketch this in as the high angle half of the (110); then subtract it from the composite (021) + (110) to obtain the low angle half of the (021), and so forth until all three peaks have been resolved. The remainder after the (002) is completed belongs to the group of peaks between 36.5° and 38.5° 2θ . Such a graphical method may lack precision, but it was adequate for this study because of the large specimen-to-specimen variation in peak shape caused by variation in grain size, chemical composition, aging condition, etc., of these fuel pins. Furthermore, in determining the $I(110)/I(021)$ ratio, peak heights were as accurate as peak areas.

Results and Conclusions

Axial Texture Gradient Measurements

Figures 4, 5, and 6 show the variation of compressive stress during heat treatment, irradiation growth, and texture versus distance from the bottom end of centrifugally bonded fuel pins. The irradiation growth was measured on the diameter of the fuel pin. A [110] texture and deficiency of [021] along the axis of the pin, $I[110]/I[021] > 1.0$, caused a shortening in length and a corresponding increase in diameter. There was also a [001] texture along the pin axis; since growth does not occur in the "c" direction, this texture causes no change in the axial dimension during irradiation. Note that the texture decreases approximately linearly with compressive stress during heat treatment from 3000 psi down to about 1000 psi; below this stress the texture is very small and seems unaffected by the stress. Irradiation tests⁴ have shown that the centrifugal bonding caused the dimensional instability of the fuel pins, and these data indicate that the texture responsible for the growth was induced by the compressive stress from the centrifuge during bonding.

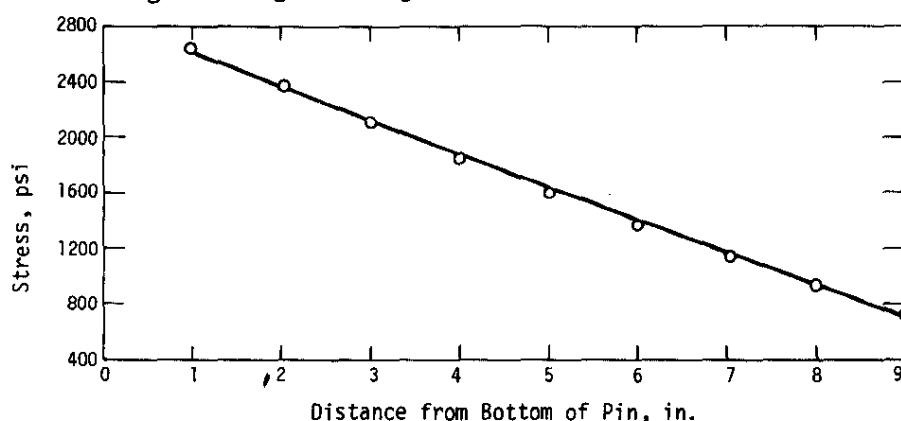


FIGURE 4 Compressive Stress During Heat Treatment of a Centrifugally Bonded Pin

(Private correspondence, A. K. Chakraborty, Idaho Nuclear Corp.)

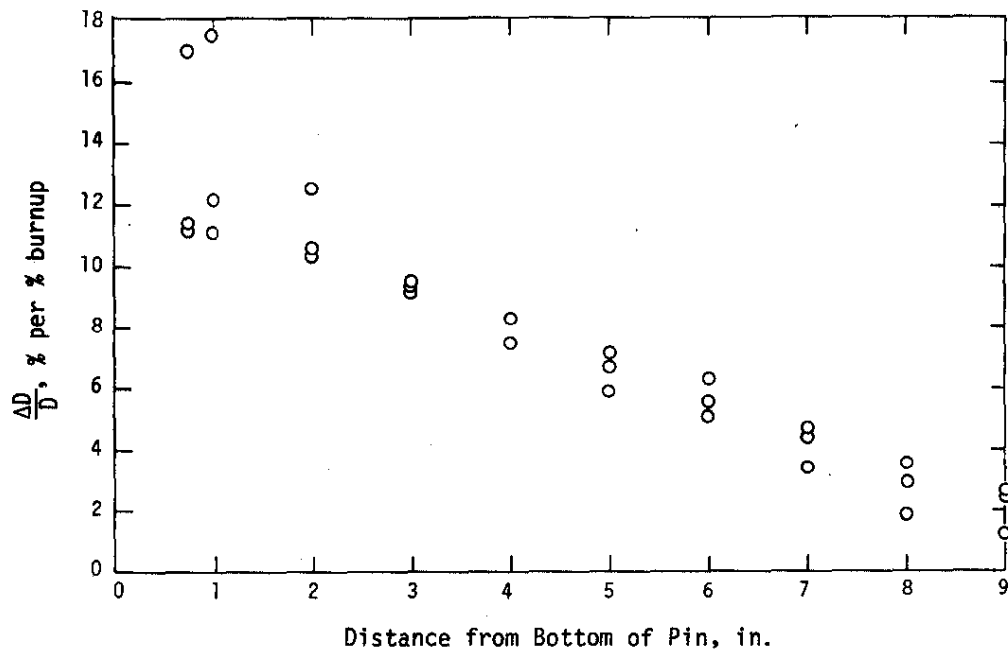


FIGURE 5 Diametrical Irradiation Growth of Centrifugally Bonded Fuel Pins
(Private correspondence, A. K. Chakraborty, Idaho Nuclear Corp.)

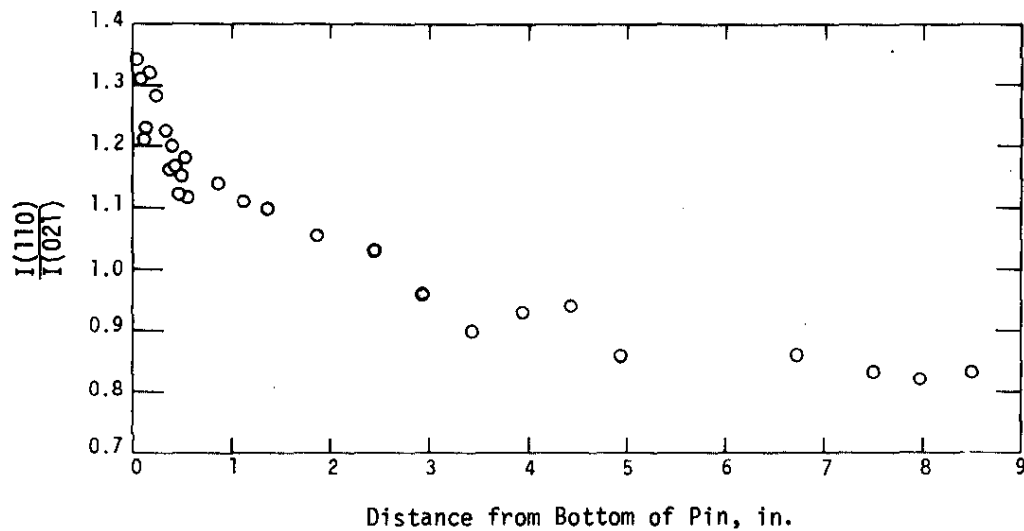
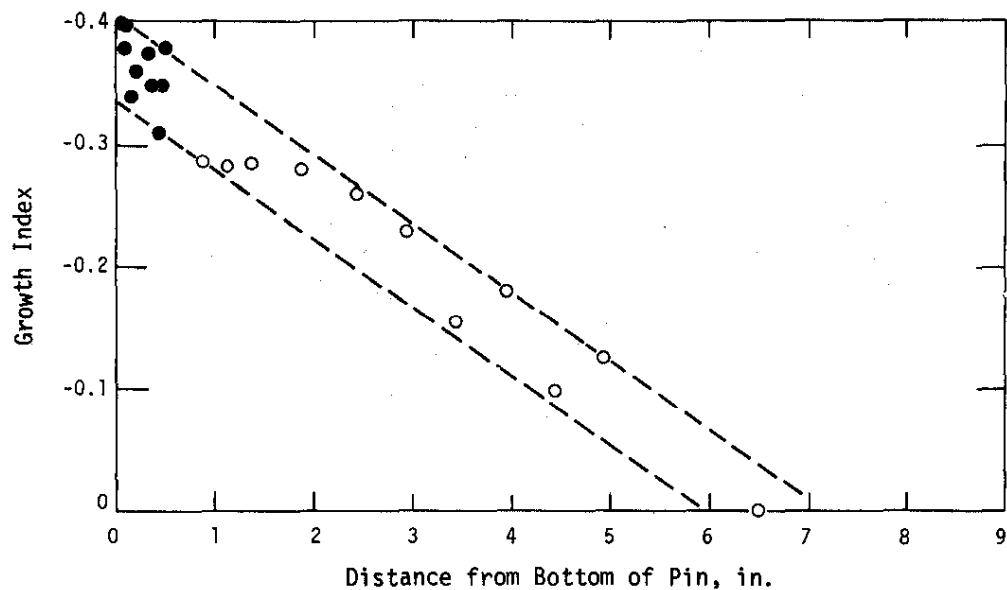


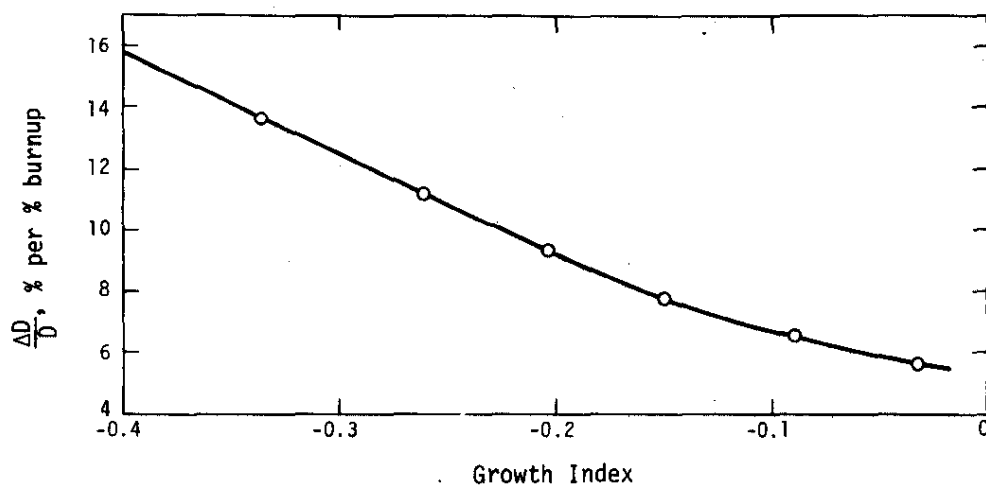
FIGURE 6 Texture Gradient in Centrifugally Bonded Fuel Pin
(Pin 41397, Batch 580)

The growth index, GI, is plotted versus the distance from the bottom of the centrifugally bonded fuel pin in Figure 7a, and the average GI values from these data are plotted as a function of diametrical irradiation growth in Figure 7b. The slope of the line in Figure 7b gives 3.32% growth per % burnup per 0.1 GI. For comparison with other investigations, these data can be normalized to single crystal growth rates as follows: The normalized growth index¹⁸ is called G_2 and $G_2 = GI/n$, where n = number of planes measured. $G_2 = 1$ for a single crystal or perfect texture. Hence, for the centrifugally bonded pins G_2 is -0.0166* because six planes were used in the present measurements. The interpretation of $G_2 = -0.0166$ is that the texture is effectively 1.66% of a perfect texture ($G_2 = 1$) or single crystal. So the growth "g" is 3.32% growth per % burnup divided by 0.0166, or $g = 200\%$ growth per % burnup per unit G_2 . Buckley¹⁷ found g for pure polycrystalline uranium to vary considerably as a function of fission rate and irradiation temperature. For the EBR-II fission rate of approximately 1×10^{14} fissions/cm³-sec (~150 watts/g) and a temperature of 500°C corresponding to the average irradiation temperature of EBR-II fuel pins, Buckley's g value for pure uranium is 500 (% growth per % burnup per unit G_2).¹⁷ Hence, the uranium-fissium g value of 200 is quite reasonable, considering that one of the main constituents of this alloy, molybdenum, lowers the growth rate^{9,10} compared to pure uranium, even in quantities as low as 500-1000 ppm. Some alloying constituents, e.g., Fe, increase the g value compared to pure uranium.¹¹ With an alloy system as complex as uranium-fissium, it will be difficult to describe how each solute element (Mo, Ru, Rh, Pd, Zr, Nb, Fe, Si, Ni) affects the growth rate as a function of temperature and fission rate.

* $G_2 = 0.1 \div 6 = 0.0166$ per 0.1 GI



a. Growth Index Variation



b. Growth Rate Versus Growth Index

FIGURE 7 Growth Rate and Growth Index for Centrifugally Bonded Fuel Pins

*Texture Measurements on End Sections and
Composite Specimens*

Table II summarizes the end-section texture data for seven centrifugally bonded fuel pins, two impact-bonded fuel pins, and two heat-treated fuel pins. The texture results are in excellent agreement with the EBR-II irradiation tests which showed that only centrifugally bonded pins shortened during irradiation. Centrifugally bonded Pins 4008, 01776, 14171, and 35424 had the small grained end under high compressive stress during bonding and have a $I(110)/I(021)$ ratio of 0.96 to 1.01. Centrifugally bonded Pins 44588, 02112, and 41397 had the large grained end under high compressive stress during bonding and had an $I(110)/I(021)$ ratio of 1.22 to 1.32. The impact-bonded and specially heat-treated pins had ratios of 0.77 to 0.80. A ratio of 0.73 represents perfectly random orientation.

Composite specimens (Figure 1) were also made from a group of transverse slices taken over 2/3 the length of each of two fuel pins. Intensities from twelve diffraction planes (hkl) were measured versus six for the other texture work, so for approximate comparison with the data of Figure 7, the GI values were divided by 2.

In these measurements a composite specimen for impact-bonded Pin 049H23 had a GI value of +0.07, and a composite specimen from impact-bonded Pin 01776 had a GI value of -0.22. These values for the composite specimens agree with the irradiation performance of fuel pins from these batches: the impact-bonded pins were stable, and the centrifugally bonded pins shortened. The value of $GI = -0.22$ for the centrifugally bonded fuel pin is in reasonable agreement with the average value of GI shown in Figure 7a, which gives individual GI values along the length of centrifugally bonded Pin 41397.

TABLE II
Texture Measurements of Bottom-End Sections
of EBR-II Fuel Pins^a

Pin	Method of Fabrication	I(110)/I(021)
049H23	Injection Cast, Impact-Bonded	0.80
38413	Injection Cast, Impact-Bonded	0.80
40971	Injection Cast, Heat-Treated at 500°C for 1 hr, Centrifugally Bonded	0.80
12367	Injection Cast, Centrifugally Bonded, Heat-Treated at 660°C 1-1/2 hr, Impact-Bonded	0.77
35424 ^b	Injection Cast, Centrifugally Bonded	1.01
01776 ^b	Injection Cast, Centrifugally Bonded	0.98
14171 ^b	Injection Cast, Centrifugally Bonded	0.98
40008 ^b	Injection Cast, Centrifugally Bonded	0.96
44588	Injection Cast, Centrifugally Bonded	1.22
02112	Injection Cast, Centrifugally Bonded	1.31
41397	Injection Cast, Centrifugally Bonded	1.32

a. End of pin which was in the bottom of the stainless steel jacket.

b. For these pins the small grained end, i.e., the top end of the casting, was the bottom end of the jacketed pin.

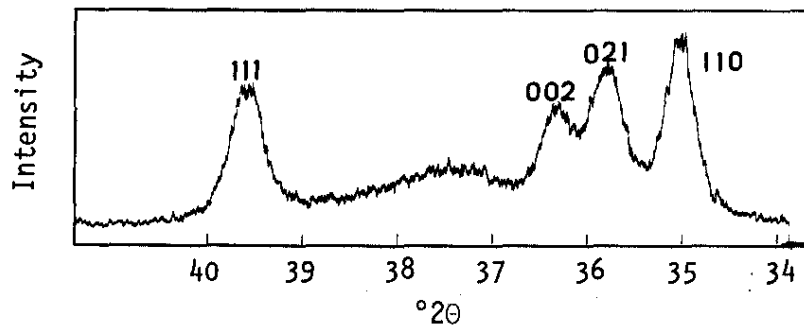
Effects of Specimen Electropolishing Solution on Texture Measurements

The cold-worked layer caused by grinding is routinely removed from the surface of X-ray diffraction specimens by electropolishing. The appearance of the microstructure of the uranium-fissium alloy after electropolishing, shown by scanning electron microscopy in Figure 11, suggests that two major phases are present, even though density, hardness, and X-ray diffraction measurements indicate that the alloy is greater than 95% alpha uranium. Both major "phases" are forms of alpha uranium, and the different microstructural appearance is due to two different modes of transformation and/or to different chemical reactions of the electropolish around the grain boundaries, where the minor phases (e.g., U_2Ru) tend to be concentrated.

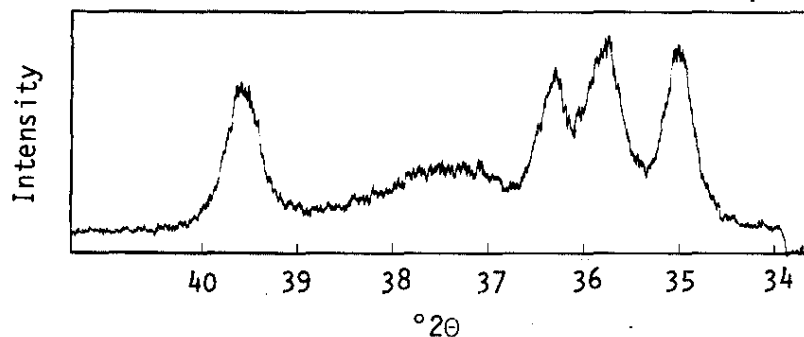
The question arises as to whether both forms of alpha uranium are textured. When electropolished with phosphoric acid, the form of alpha uranium around the grain boundaries is in relief, and hence contributes less to the diffraction intensities because it is slightly below the plane of diffraction in the diffractometer. This relative relief of the two forms of uranium was used to determine the relative contribution of the two forms of alpha uranium to the measured diffraction intensities by grinding and electropolishing the same specimen (the bottom end of Pin 02112) cast and centrifugally bonded twice using a different electropolish each time. The X-ray scans are shown in Figure 8. The intensities of the alpha-uranium triplet indicate that the scan from the surface more uniformly polished with chromic-acetic acid is less textured; thus the grain boundary region is less textured than the matrix. Hence if the chromic-acetic polish had been used instead of the phosphoric acid polish, the GI values would be have been slightly smaller and g slightly larger.

Metallography microprobe, and hardness observations indicate that in the grain boundary region the form and amount of alloying constituents are different; these differences may have caused the difference in texture. There is also evidence from work on other uranium alloys¹⁸ that the amount and kind of alloying constituent affect the susceptibility of a material to stress-induced texture.

From the conclusion that the grain-boundary alpha phase is less textured than the matrix grains, it follows that less texture will be induced in pins that have the small-grained end under high compressive stress during centrifuging, since there is more grain boundary phase in the small-grained end of the pin. This was observed for Pins 01776, 40008, 14171, and 35424 (Table II).



a. Standard Phosphoric Acid Electropolish
(Grain Boundary Alpha Phase Preferentially
Removed)



b. Chromic-Acetic Acid Electropolish
(A More Uniform Electropolish)

FIGURE 8 Effect of Electropolish on Diffraction
Intensities of EBR-II Fuel Pins

Note that in going from condition a to condition b the $I(110)/I(021)$ ratio decreased from 1.15 to 0.95 and $I(002)$ increased toward random orientation.

Line Broadening and Lattice Contraction

Compared to pure uranium, the alpha-phase diffraction lines of the uranium-fissium fuel pins are broadened, and the orthorhombic alpha lattice is contracted approximately 0.05Å in the [010] direction (Figure 3). In general, the diffraction lines of the centrifugally bonded fuel pins are broadened much more than the impact-bonded pins or the specially heat-treated pins.

With regard to lattice contractions, the (oko)-type reflections of both centrifugally bonded and impact-bonded pins are shifted to higher 2θ values; for example, (020) is shifted from 30.46° to 30.75° , and the (021) is shifted from 35.55° to 35.75° . Delaplace¹⁹ observed similar [010] lattice contractions (0.03Å) for uranium-1.15 wt % molybdenum cooled at rates greater than 400°C per sec. The lattice parameter returned to its normal value after this alloy was annealed for 50 hours at 500°C .

MICROSTRUCTURE AND HARDNESS OF FUEL PINS

Experimental Procedure

Surface preparation for microstructure and hardness analyses was the same as for X-ray diffraction. Replica electron microscopy was performed on an RCA Model EMU microscope. The specimens were prepared by replicating with "Formvar"* backed by "Parlodion"*** and shadowed with uranium. Scanning electron microscopy was performed on the Cambridge Stereoscan Mark IIa microscope. Quantitative microanalysis for U, Mo, and Ru was performed on a Model 400 microprobe manufactured by the Materials Analysis Corporation. Microhardness was measured on a Tukon Hardness Tester using a 100-g load and a Vickers diamond pyramid indenter.

Results

Hardness Measurements

The Vickers diamond pyramid hardness (DPH) values for an as-cast pin, a centrifugally bonded pin, and an impact-bonded pin are summarized in Table III. In the bonded pins the hardness of both the grain boundary region, which appears to be a different form of alpha uranium, and the matrix was measured. The hardness of the matrix is the same for both centrifugally bonded and impact-bonded pins; however, the region around the grain boundary, softer in both pins, is softest for the impact-bonded pins. This difference confirms the microstructural observations that the impact-bonded grain boundary region is more aged, i.e., closer to the equilibrium unstrained structure.

Even though there is a variation of hardness between the matrix and grain boundary regions (640 to 556) of the bonded pins, all the values correspond to the alpha phase of uranium; the value for the as-cast pin corresponds to the hardness of gamma uranium (232).

* Registered tradename of Shawinigan Products Corp.

** Registered tradename of Mallinckrodt Chemical Co.

Microstructure Studies

The microstructures of the impact-bonded and centrifugally bonded fuel pins, Figures 9 and 10, have some common features and some differences. Both fuel pins show small grains at the top and larger grains at the bottom end of the pin, when referenced to the as-cast condition, because the pins are cooled from the top after injection casting. However, both large- and small-grained ends of the fuel pins were located in the bottom end of the stainless steel jackets. The bottom end of the jacketed pin is the end that received the high stresses during centrifuge bonding.

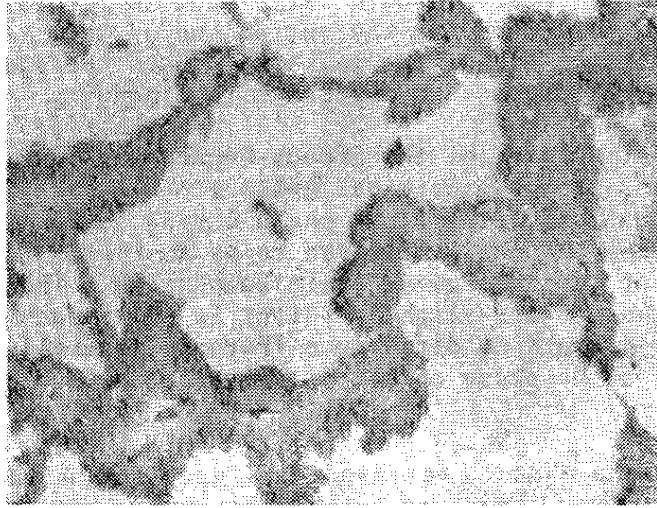
The microstructures of the impact-bonded and centrifugally bonded fuel pins show the original gamma grain boundaries, even after transformation to the alpha phase during bonding. Both types of pins also show the phase believed to be another form of alpha uranium adjacent to these gamma grain boundaries. These regions appear more aged and are slightly softer in the impact-bonded pins. Because of the grain size difference there is generally more of the grain-boundary alpha phase on the small-grained end of the pins.

Scanning micrographs (Figures 11 and 12) show the two forms of distorted alpha phase: equiaxed dark gray grains and an acicular, light gray structure around the grain boundaries. The white phase that delineates the original gamma grain boundaries is believed to be U_2Ru . The randomly dispersed, star-shaped precipitates were found by microprobe analysis to be zirconium rich. These micrographs also clearly show that the grain boundary alpha regions are preferentially removed during electropolishing.

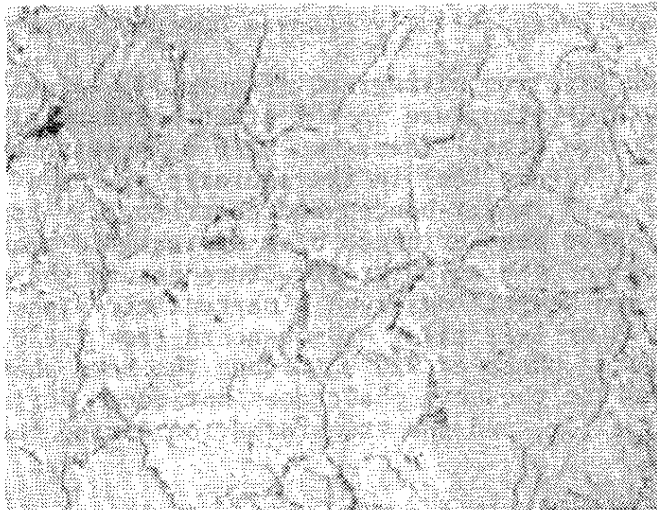
The replica electron micrograph (Figure 13a) gives the best view of the acicular structure in the grain boundary alpha region of the impact-bonded pins. There was also some evidence of a banded structure (Figure 13b) in the equiaxed grains of the large grained ends of both impact-bonded and centrifugally bonded pins. These bands may have been evidence of a martensitic transformation or a coarser form of the acicular structure around the grain boundaries. Zegler and Nevitt⁶ observed a martensitic alpha structure, but only in a U-3 wt % Fs alloy H_2O -quenched from $720^\circ C$. This alloy goes from the gamma phase at $720^\circ C$ through the beta phase to the alpha phase, whereas the beta phase does not occur during cooling of the U-5 wt % Fs alloy, and the transformation during bonding is from gamma to alpha.

Harding and Waldron¹¹ have also observed decomposition structures of gamma phase uranium alloys (10 atom % Ti, Nb, Zn, Mo), with differing metallographic appearance, that exhibited a similar X-ray lattice contraction to the U-Fs alloy. The structures were designated "distorted α " since there was a contraction in the b-direction of the normal orthorhombic α cell. The dif-

ference in appearance is attributed to transformation both by a shear and a nucleation and growth mechanism. The type of transformation produced depended upon the composition, the cooling rate from γ phase, and the effect of the solute element on the decomposition rate of the metastable gamma phase.

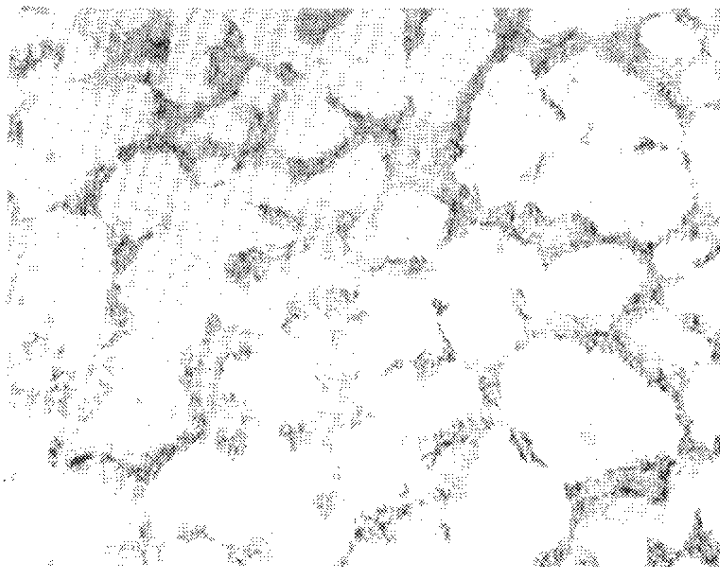


a. Top End of Fuel Pin 38413 (bottom end of the casting)

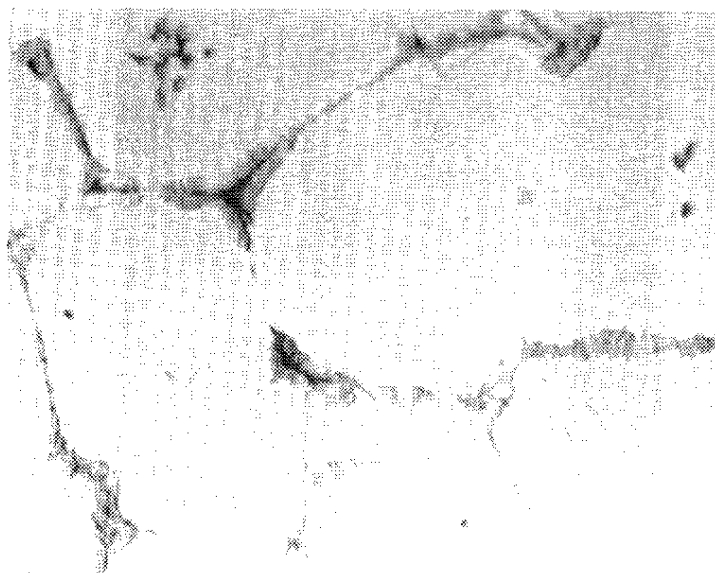


b. Bottom End of Fuel Pin 38413 (top end of the casting)

FIGURE 9 Optical Micrographs of Impact-Bonded Fuel Pin (1000X)

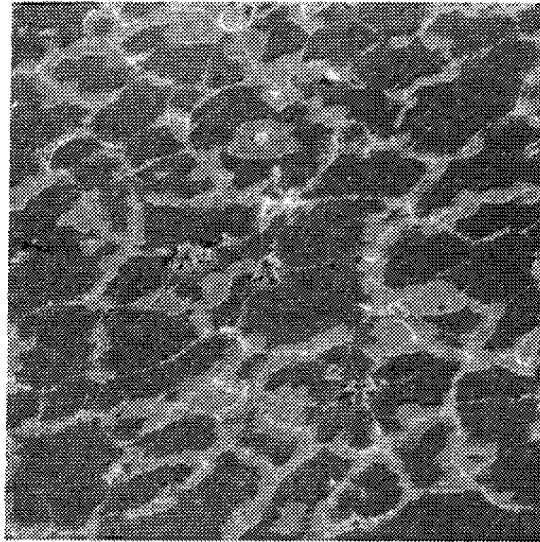


a. Top End of Fuel Pin 44588 and Casting

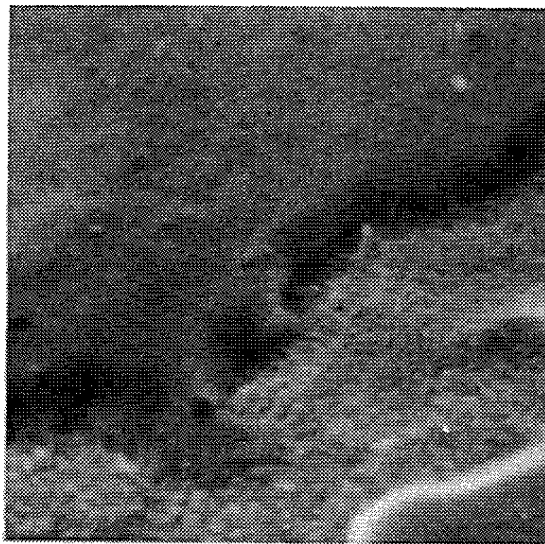


b. Bottom End of Fuel Pin 44588 and Casting

FIGURE 10 Optical Micrographs of Centrifugally Bonded Fuel Pin (1000X)



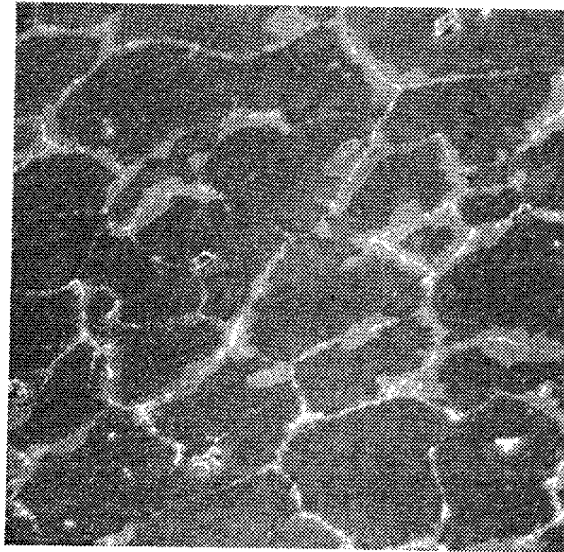
1000X



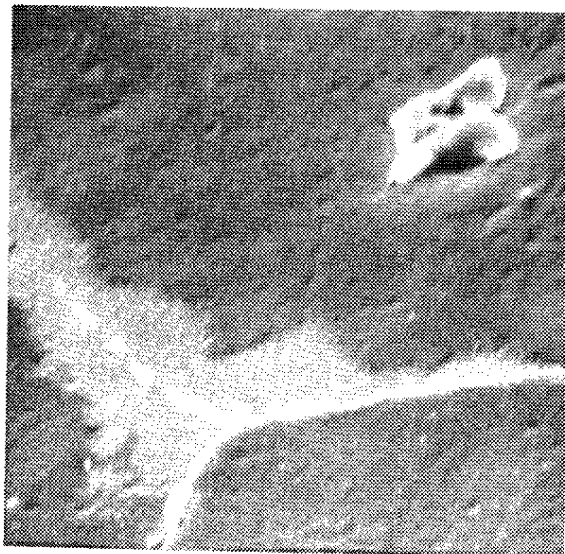
20,000X

FIGURE 11 Scanning Electron Micrographs of
Impact-Bonded Fuel Pin

Section from the bottom end of fuel
pin 38413, but the top (small grain)
end of the casting.



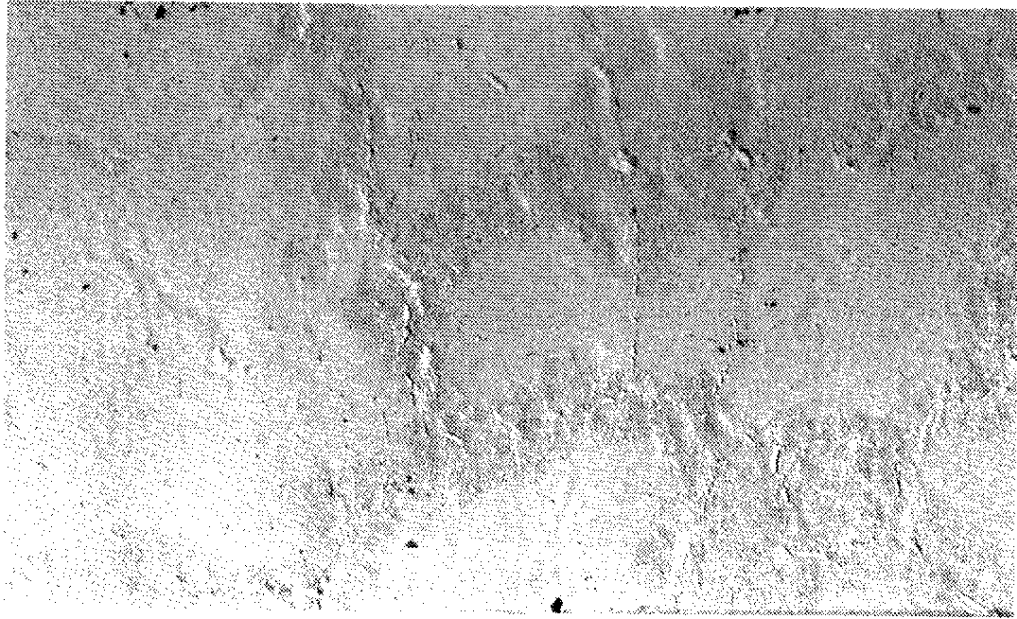
1000X



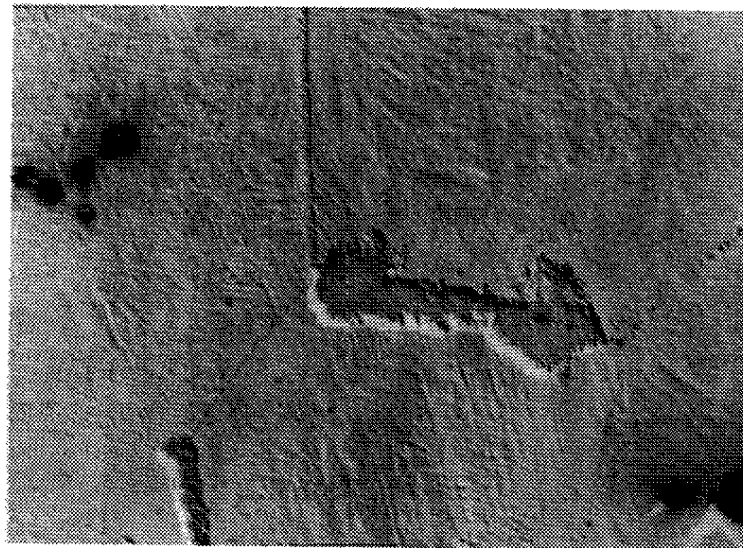
5000X

FIGURE 12 Scanning Electron Micrograph of
Centrifugally Bonded Fuel Pin

Section from bottom end of fuel
pin 40008, but the top end of
the casting.



a. Impact-Bonded Pin 38413, Small Grained End of Casting (3500X)



b. Centrifugally Bonded Pin 44588, Large Grained End of Casting (1600X)

FIGURE 13 Replica Micrographs of Grain boundary and Matrix Structure of Impact-Bonded and Centrifugally Bonded Pins

Electron Probe Micro-Analysis

Probe studies of impact-bonded and centrifugally bonded pins showed that more molybdenum than ruthenium was in the matrix, and more ruthenium than molybdenum was in the grain boundary region. The studies also showed that the star-shaped particles (Figure 11) were zirconium rich.

MECHANISM FOR STRESS-INDUCED TEXTURE

It is believed that the mechanism proposed by Riggs and Neumann¹⁸ to explain texture induced in cylinders of uranium end-quenched from the beta phase is applicable to this case; namely, that the texture formation is a stress-relieving mechanism in which grains are oriented during nucleation and growth of the alpha phase such that the "weaker" bonds of the [010] crystallographic directions are parallel to the directions of the tensile stress. The reasons for choosing this mechanism follow.

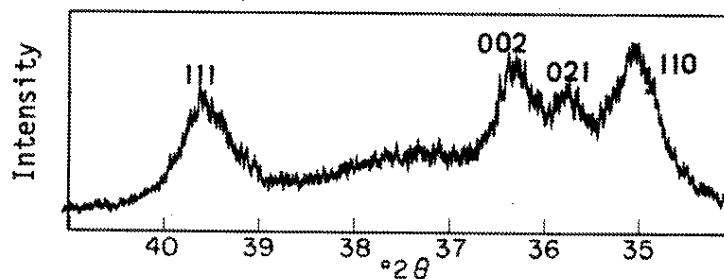
Texture Profiles

The centrifugally bonded pins have a texture profile similar to the end-quenched uranium cylinders (Figure 14), i.e., a [001], [110] axial texture and a deficiency of [021] at the high-stress end of the pin. As the distance from the end increases, the [110] decreases, the [001] increases, and the [021] remains deficient.

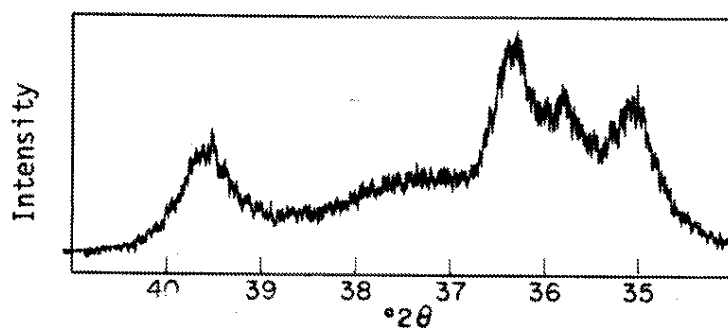
Source of Stress

For the end-quenched cylinder of uranium, the sources of stress are the thermal stresses and the stresses due to the volume change during the $\beta \rightarrow \alpha$ transformation. The stress at the transformation interface increases with cooling rate; hence it is maximum at the end of the cylinder.

For the centrifugally bonded pins, the principal source of stress is the stress from the centrifuge. The thermal stresses should be small and relieved quickly, because the $\gamma \rightarrow \alpha$ transformation occurs at high temperature (500°C) where the thermal energy of the structure is high. Furthermore, the stress due to volume change during the $\gamma \rightarrow \alpha$ transformation should be small because the γ phase has a lower yield strength (see hardness values, Table III) than the alpha phase.



a. Bottom End of Pin 41397



b. 1/2 in. from Bottom End of Pin 41397

FIGURE 14 Variation of Texture Along the Length of Centrifugally Bonded Pins

Note the increase in $I(002)$ and the decrease in $I(110)/I(021)$ from a to b. This type of variation has been observed in end-quenched uranium cylinders.¹⁸

TABLE III

DPH Values for Uranium-Fissium Fuel Pins^a

	DPH Value
Injection Cast	232
Injection Cast and Centrifugally Bonded	
Matrix	640
Grain-boundary regions	584
Injection Cast and Impact-Bonded	
Matrix	635
Grain-boundary regions	556

a. Tukon hardness tester, 100-g load, Vickers diamond pyramid indenter. Each value is the average of measurements in 5 areas.

Magnitude of Stress

For the end-quenched cylinders of uranium, in which the $\beta \rightarrow \alpha$ transformation of rapidly cooling uranium occurs at 600°C or lower, the beta phase can exert stresses of 6000 psi or greater on the alpha phase before the alpha phase yields. The maximum stress for the centrifugally bonded pins was about 3000 psi. In agreement with the higher stress level, there was more texture developed in the end-quenched uranium alloys¹⁸ than in the centrifugally bonded pins.

Direction of Stress

For the end-quenched uranium alloys, Riggs and Neumann assumed the transformation interface to be a plane perpendicular to the cylinder axis, so the stress occurred on a cross section. Under these conditions the alpha phase transformation front was subjected to radial tension while the adjoining beta phase was in radial compression. For the centrifugally bonded pins, the radial direction of the pin was also in tension during $\gamma \rightarrow \alpha$ transformation so alignment of the weaker bonds of the [010] direction parallel to the direction of tensile stress would also provide the greatest stress relief during transformation.

Other Mechanisms for Stress-Induced Texture

For the end-quenched uranium alloys, Riggs and Neumann considered that textures were induced by plastic deformation of the alpha phase by the beta phase, but concluded that slip would require too much elongation to produce the large reorientation required. A twinning deformation mechanism would give a large reorientation, but the volume fraction of twinned material was too small.

For the centrifugally bonded pins there was no twinning. There is, however, a possibility that the banded structure in the equiaxed grains of Figure 13b is produced by the centrifuge stress causing shear to occur more easily on one set of planes, as proposed in Reference 4.

ACKNOWLEDGMENTS

The authors are grateful to Drs. C. M. Walter and A. K. Chakraborty of the ANL Idaho Facility for the specimens and the irradiation test data, to C. W. Krapp and T. L. Gill for assistance with the X-ray and metallographic measurements and to A. E. Symonds for the microprobe studies.

REFERENCES

1. J. P. Bacca, M. J. Feldman, C. C. McClellan, C. M. Walter, and S. T. Zegler. "Anomalous Irradiation Performance of Centrifugally Bonded EBR-II Driver Fuel." *ANS Trans.* 12, 555 (1969).
2. C. R. Hann and R. D. Leggett. "Postirradiation Examination of Centrifugally Bonded EBR-II Driver Fuel." *ANS Trans.* 12, 555 (1969).
3. C. M. Walter, M. H. Mueller, and J. P. Bacca. "Application of X-ray Texture Studies to Explain the Anomalous Performance of Centrifugally Bonded EBR-II Driver Fuel." *ANS Trans.* 13, 95 (1970).
4. C. M. Walter, A. K. Chakraborty, J. P. Bacca, and P. G. Shewmon. "Anisotropic Irradiation Growth of EBR-II Driver Fuel Pins." *J. Nucl. Mat.* 39(1), 122 (1971).
5. M. V. Nevitt and S. T. Zegler. "Transformation Temperatures and Structures in Uranium-Fissium Alloys." *J. Nucl. Mat.* 1, 6 (1959).
6. S. T. Zegler and M. V. Nevitt. *Structures and Properties of Uranium-Fissium Alloys*. USAEC Report ANL-6116, Argonne National Laboratory, Argonne, Ill. (1961).
7. E. F. Sturcken. *An X-ray Method for Predicting the Stability of Natural Uranium at Low Burnup*. USAEC Report DP-251, E. I. du Pont de Nemours & Co., Savannah River Laboratory, Aiken, S. C. (1957); E. F. Sturcken and W. R. McDonell. "An X-ray Method for Predicting Anisotropic Irradiation Growth in Uranium." *J. Nucl. Mat.* 7, 85 (1962).
8. S. H. Paine and J. H. Kittel. *Preliminary Analysis of Fission-Induced Dimensional Changes in Single Crystals of Uranium*. USAEC Report ANL-5676, Argonne National Laboratory, Argonne, Ill. (1958).
9. W. R. McDonell, W. N. Rankin, R. T. Huntoon. "Effect of Alloying Additions on Anisotropic Growth of Uranium." *J. Instit. Metals* 97, 26 (1969).
10. J. L. Baron and R. Cadalbert. "Influence Specifique D'additions A L'uranium Sur La Croissance En Pile." *J. Nucl. Mat.* 36, 123 (1970).

11. A. G. Harding and M. B. Waldron. *Transformations in Uranium Alloys with High Solute Solubility in the B. C. C. γ Phase, Part 1.* UKAEA Report AERE M/R 2673, Atomic Energy Research Establishment, Hartwell, England (1958).
12. R. N. Thudium. *A Study of Cold Work Effects on Grinding of a Sample Surface.* USAEC Report NLCO-804, National Lead Co., Cincinnati, Ohio (1959) p. 59-60.
13. E. F. Sturcken. "Status of the Growth Index Formalism." *Papers and Discussions from the X-ray Preferred Orientation Meeting, Argonne National Laboratory, Dec. 15-16, 1960.* USAEC Report ANL-6359, Argonne National Laboratory, Argonne, Ill. (1960) p. 20-34.
14. P. R. Morris. "Reducing the Effects of Nonuniform Pole Distribution in Inverse Pole Figure Studies." *J. Appl. Phys.* 30, 595 (1959).
15. E. F. Sturcken. *Determination of Theoretical Diffraction Intensities for Alpha Uranium.* USAEC Report NLCO-804, National Lead Co., Cincinnati, Ohio (1960) p. 49-58.
16. E. F. Sturcken. *A Generalized Growth Index Formalism.* USAEC Report NLCO-804, National Lead Co., Cincinnati, Ohio (1960) pp 9-24; see also E. F. Sturcken and J. W. Croach. "Predicting Physical Properties in Oriented Metals." *Trans. AIME* 227, 934 (1963).
17. S. N. Buckley. *Irradiation Growth in Uranium.* UKAEA Report AERE-R-5262, Atomic Energy Research Establishment, Hartwell, England (1966).
18. K. R. Riggs and N. F. Neumann. *Effect of Alloy Additions on the Quench-Induced Texture of Alpha-Uranium.* USAEC Report MCW-1491, Mallinckrodt Chemical Works, Weldon Springs, Mo. (1965).
19. J. Delaplace. "Comparison of the Influence of Small Additions of Chromium, Iron or Molybdenum on the Transformations Undergone by Uranium During Quench and Subsequent Annealing." *Mem. Sci. R. de Met.* 57, 721 (1960).